Optical Materials 82 (2018) 60–64

Contents lists available at ScienceDirect

Optical Materials

journal homepage: www.elsevier.com/locate/optmat

Scintillation and dosimetric properties of Ce-doped ^{6}LiF-CaF_2 eutectic composites

Naoki Kawano[a,*], Noriaki Kawaguchi[b], Kentaro Fukuda[c], Go Okada[b], Takayuki Yanagida[b]

[a] Graduate School of Engineering Science, Akita University, 1-1Tegata Gakuen-machi, Akita, 010-8502, Japan
[b] Graduate School of Materials Science, Nara Institute of Science and Technology, 8916-5, Takayama, Ikoma, Nara, 630-0192, Japan
[c] Tokuyama Corporation, 1-1, Mikage-cyo, Shunan-shi, Yamaguchi, 745-8648, Japan

ARTICLE INFO

Keywords:
Scintillation
TSL
OSL
Ce^{3+}
LiF
CaF_2

ABSTRACT

Scintillation and dosimetric properties of ^{6}LiF-CaF_2 eutectic composites doped with different concentrations of Ce (0, 0.1 and 0.5%) were investigated. The Ce-doped samples showed scintillation due to the 5 d-4f transitions of Ce^{3+} and self-trapped excitons (STE) at 320–340 and 300 nm, respectively. Furthermore, the Ce-doped samples exhibited thermally-stimulated luminescence (TSL) with glow peaks around 150 °C after X-ray irradiation of 1000 mGy. The TSL response of the 0.5% Ce-doped sample increased monotonically with X-ray dose over a dose range of 0.1–1000 mGy. Moreover, the Ce-doped samples showed optically-stimulated luminescence (OSL) with peaks at 320–340 nm due to the 5 d-4f transitions of Ce^{3+} under 630 nm stimulation light after X-ray irradiation of 1000 mGy.

1. Introduction

Phosphor materials have been attracted much attention in various fields of ionizing radiation, and they can be classified into two types: scintillator and dosimeter phosphors. The former converts absorbed energy of a single quantum (keV-GeV) into low energy photons immediately, and has been used in a wide range of application fields such as nuclear medicine [1], well-logging [2] and border security [3]. The basic requirements for many applications are high light yield, fast decay, high density and high radiation tolerance. On the other hand, the latter storages the absorbed energy for several weeks and releases the energy by thermal (thermally-stimulated luminescence, TSL) or optical (optically-stimulated luminescence, OSL) stimulation. The main application of TSL and OSL is individual radiation monitoring [4]. In this application, the effective atomic number of the materials are expected to be close that of the biological tissue (Z_{eff} = 7.35–7.65) [5], because interaction probability of ionizing radiations with matter depends on the chemical composition of materials. Up to now, many researchers investigate scintillation and dosimetric properties of various kinds of materials such as oxide [6,7], fluoride [8] and iodide [9].

Among the materials above, fluoride is one of the most widely used materials as scintillators and dosimeters. $LiCaAlF_6$ crystal doped with Eu and Ce is one of the example as neutron scintillators [10], and it is commercialized by Tokuyama Corp. In this compound, ^{6}Li is incorporated to detect thermal neutrons because ^{6}Li has a high interaction probability with thermal neutrons due to the nuclear reaction of ^{6}Li (n, α)^{3}H. Besides, Eu-doped CaF_2 has been focused on as scintillators in search for dark matter [11] because ^{19}F has the best figure of advantage for spin coupled dark matter search [12]. Furthermore, LiF doped with Mg, Ti has been used as TSL dosimeters. The TSL response is linear against irradiation dose with the dynamic range of 20 μGy–10 Gy [1]. In addition to LiF, Mn-doped CaF_2 is equipped in another commercial dosimeter (TLD-400), and it shows a glow peak at 260 °C with a linear dose response function over 0.5 mGy – a few kGy [13].

Recently, LiF-CaF_2 eutectic compounds have been focused on for scintillator and dosimeter applications. This eutectic system of LiF-CaF_2 can be formed at the eutectic composition (LiF:CaF_2 = 80:20 mol%) [14–22]. In general, eutectic compounds have excellent bonding between different phases with better mechanical properties and thermal shock resistance than those of single crystals and conventional ceramics [14,15]. Up to now, scintillation properties of Eu-doped ^{6}LiF-CaF_2 have been investigated for neutron scintillators. Furthermore, the effective atomic number of LiF-CaF_2 eutectic compounds (Z_{eff} = 9.86) is close to that of the soft tissue of human body (Z_{eff} = 7.35–7.65) [5]. Therefore, LiF-CaF_2 eutectic compounds are a promising candidate for individual dosimetry applications. In the past research, Mn-doped LiF-CaF_2 eutectic composite is first proposed for dosimeter applications [15].

In the present study, we fabricated ^{6}LiF-CaF_2 eutectic compounds with different concentrations of Ce. To the best of our knowledge, there

* Corresponding author.
E-mail address: n-kawano@gipc.akita-u.ac.jp (N. Kawano).

https://doi.org/10.1016/j.optmat.2018.05.027
Received 5 April 2018; Received in revised form 7 May 2018; Accepted 8 May 2018
Available online 29 May 2018
0925-3467/

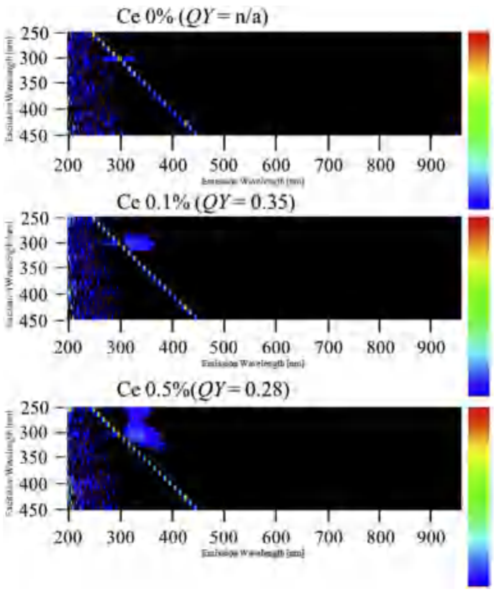

Fig. 1. PL excitation/emission contour graphs of non-doped and Ce-doped ^{6}LiF/CaF_2.

are no research article reporting dosimeter properties of Ce-doped ^{6}LiF-CaF_2 eutectic compounds. Dosimeter properties can be enhanced by an incorporation of Ce based on the past study [23]. After the synthesis of the eutectic compounds, we investigated photoluminescence (PL) and scintillation properties. Following these characterizations, storage luminescence properties such as TSL and OSL were also evaluated for dosimeter applications. It should be noted that it is important to study both scintillation and dosimeter properties comprehensively because some materials such as Ce-doped CaF_2 show a complementary relationship between these two properties [23].

2. Experimental methods

High purity (99.99%) fluoride powders of ^{6}LiF (95% enriched), CaF_2 and CeF_3 were used as the starting materials. The ^{6}LiF and CaF_2 were mixed at 80:20 M ratio, which corresponds to the eutectic composition, and a fraction of CeF_3 was added (0.1 mol%, 0.5 mol% with respect to that of CaF_2). These materials were loaded into a graphite crucible, and the micro-Bridgman method was used to produce Ce-doped ^{6}LiF-CaF_2 [16]. The crucible was placed and surrounded by carbon resist heaters inside a stainless chamber. The crucible was heated up to 400 °C and kept for about 8 h in vacuum (10^{-4} Torr). After the baking, the chamber was filled with high purity Ar (99.999%) and CF_4 (99.999%) gases until ambient pressure. The ratio of Ar and CF_4 was 9:1. Further, the crucible was heated up to 800 °C and then kept for 30 min. Finally, the heater was stopped and cooled to room temperature with a cooling rate of 5 °C/min.

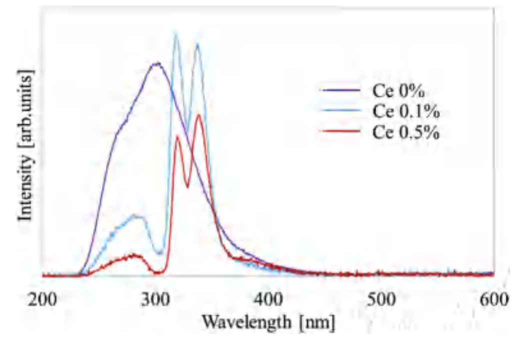

Fig. 3. X-ray irradiated scintillation spectra of non-doped and Ce-doped ^{6}LiF/CaF_2.

Quantum yield (*QY*) values and PL excitation/emission contour graphs were measured by using Quantaurus-QY (C11347, Hamamatsu Photonics). PL decay time profiles were evaluated by using Quantaurus-τ (C11367, Hamamatsu Photonics). In the measurement, the excitation wavelength was 280 nm, and the monitoring wavelength was 335 nm. As scintillation properties, X-ray-induced scintillation spectra were measured using our original setup [24]. The X-ray source was an ordinary X-ray tube having a tungsten anode target and beryllium window. For X-ray irradiation, the X-ray tube was operated by applying the bias voltage of 40 kV and tube current of 1.2 mA. Scintillation decay time profiles were measured by the pulse X-ray equipped afterglow characterization system, equipped with a pulse X-ray source [25]. The spectral sensitivity of photomultiplier tube (PMT) used in this measurement covered from 160 to 650 nm. For TSL, TSL glow curves were measured by using a TSL reader (TL-2000, Nanogray) with a heating rate of 1 °C/s over from 50 to 490 °C [26]. For OSL, OSL spectra were measured under 630 nm stimulation by using Quantaurus-τ (Hamamatsu Photonics).

3. Results and discussion

Fig. 1 illustrates PL excitation/emission contour graphs of non-doped and Ce-doped ^{6}LiF-CaF_2. The 0.1% and 0.5% Ce-dope samples exhibited emissions at 320 and 340 nm under the excitation wavelengths across 280–320 nm while no emission was observed in the non-doped sample. The emission wavelengths of the 0.1% and 0.5% Ce-doped samples agreed well with reported values for Ce-doped CaF_2 in the past study [23]. Thus, these emissions were attributed to the 5 d-4f transitions of Ce^{3+} [23]. In addition, *QY* values of non-doped and Ce-doped ^{6}LiF-CaF_2 are also indicated in Fig. 1. The *QY* values were n/a (0% Ce), 0.35 (0.1% Ce) and 0.28 (0.5% Ce). The *QY* value of the 0.1% Ce-doped sample was almost comparable to that of other 0.1% Ce-doped fluorides such as MgF_2 and $LiSrAlF_6$ [27,28].

Fig. 2 represents PL decay time profiles of non-doped and Ce-doped ^{6}LiF-CaF_2. The excitation wavelength was 280 nm, and the monitoring wavelength was 335 nm. Each decay curve was approximated by an

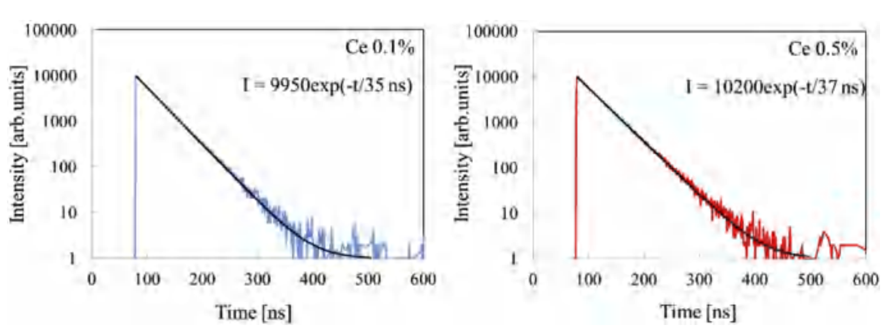

Fig. 2. PL decay time profiles of Ce-doped ^{6}LiF/CaF_2. Excitation wavelength was 280 nm, and monitoring wavelength was 335 nm.

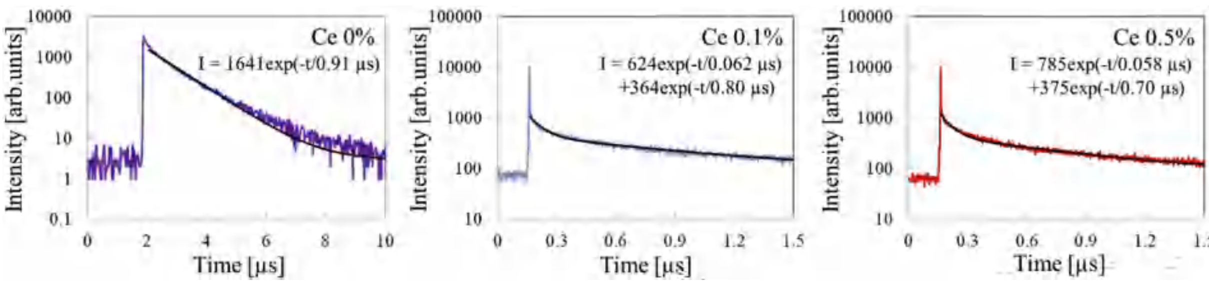

Fig. 4. X-ray irradiated scintillation decay time profiles of non-doped and Ce-doped $^{6}LiF/CaF_2$.

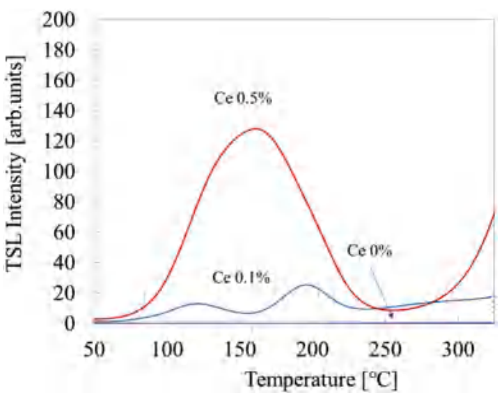

Fig. 5. TSL glow curves of non-doped and Ce-doped $^{6}LiF/CaF_2$ after X-ray irradiation of 1000 mGy. The heating rate was 1 °C/s, and the spectral sensitivity of PMT covered from 160 to 650 nm.

Table 1
Maximum peak temperature and activation energy.

Peak temperature [°C]		Activation Energy [eV]
Ce 0.1%	120	0.65
	197	0.81
Ce 0.5%	140	0.65
	177	0.75

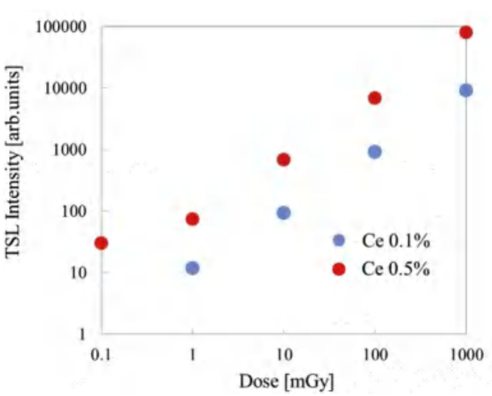

Fig. 6. TSL dose response curves of Ce-doped $^{6}LiF/CaF_2$.

exponential decay function. The signal from the non-doped sample could not be detected. The PL decay times were 35 ns (0.1% Ce), 37 ns (0.5% Ce). The PL decay time constants were typical constant of the 5 d-4f transitions of Ce^{3+} [27,28]. Thus, the origin of the component was the 5 d-4f transitions of Ce^{3+}. The PL decay time was almost constant, regardless of Ce concentrations.

Fig. 3 shows X-ray induced scintillation spectra of non-doped and Ce-doped ^{6}LiF-CaF_2. The non-doped sample showed scintillation with a broad peak around 300 nm. The broad peak may be ascribed to self-trapped excitons (STE) from the past studies [29,30]. Further, sharp peaks at 320 and 340 nm were observed in the 0.1% and 0.5% Ce-doped samples. These spectral features agreed well with that in PL. Thus, the emissions were due to the 5 d-4f transitions of Ce^{3+}. The scintillation intensity of the 0.1% Ce-doped sample was higher than that of the 0.5% Ce-doped sample, which was consistent with PL intensity.

Fig. 4 represents X-ray induced scintillation decay time profiles of non-doped and Ce-doped ^{6}LiF-CaF_2. Each decay curve was approximated by exponential decay functions to derive the decay times. The obtained value for the non-doped sample was 0.91 μs. The component might be attributed to STE in ^{6}LiF-CaF_2 host from the past studies [29,30]. In additions, the decay times of the 0.1% and 0.5% Ce-doped samples were 62 ns and 0.80 μs (0.1% Ce), 58 ns and 0.70 μs (0.5% Ce), respectively. The decay time constants of the faster component were comparable to typical values of 5 d-4f transitions of Ce^{3+} observed in other Ce-doped materials [29,31]. Thus, the component was attributed to the 5 d-4f transitions of Ce^{3+}. In addition, the origin of the slower component might be ascribed to STE in the ^{6}LiF-CaF_2 host based on the past studies [29,30]. The decay time constants of two components were almost the same, regardless of the concentrations of Ce.

Fig. 5 shows TSL glow curves of non-doped and Ce-doped ^{6}LiF-CaF_2. The TSL glow curves were measured after X-rays irradiation of the samples (1000 mGy). The 0.1% Ce-doped sample showed two TSL glow peaks around 130 and 180 °C, and the 0.5% Ce-doped sample showed a broad TSL peak at 150 °C. The origin of these TSL glow peaks might be attributed to LiF host or some unknown impurities in the starting materials [15]. In addition, the TSL intensity for the 0.5% Ce-doped sample was higher than that for 0.1% Ce-doped sample while the scintillation intensity for the 0.5% Ce-doped sample was lower than that for 0.1% Ce-doped sample. This complimentary relation between scintillation and TSL intensity could be also observed in Eu-doped LiCaAlF$_6$ [32]. Moreover, maximum glow peak temperature and activation energy were calculated to evaluate trap depth. These factors were derived by numerical approximation assuming the first-order kinetics [33]. These results are summarized in Table 1. The TSL intensity for the non-doped sample was too low to evaluate these parameters accurately. The activation energy was almost constant regardless of Ce concentrations. Therefore, it is suggested that the trap was created by Ce doping. Fig. 6 shows dose response curves of Ce-doped ^{6}LiF-CaF_2. The integrated value of the observed glow peaks was considered as a TSL signal. The detected lower limit was found to be 1.0 mGy (0.1% Ce) and 0.1 mGy (0.5% Ce). The limit of the 0.5% Ce-doped sample was higher than that of TSL materials such as LiF doped with Mg and Ti (20 μGy) and $Li_2B_4O_7$ doped with Cu (10 μGy) [4]. Furthermore, the 0.1% and 0.5% Ce-doped samples had a linear response against the X-ray dose over the dose range of 1–1000 mGy (0.1% Ce) and 0.1–1000 mGy (0.5% Ce). It should be noticed here that the TSL signal was so strong that the signal saturated in the TSL reader above 1000 mGy. Based on these results, it is confirmed that the 0.5% Ce-doped sample showed a high TSL dosimeter performance.

In order to investigate deeper traps, we evaluated OSL properties. Fig. 7 represents OSL decay time profiles of Ce-doped ^{6}LiF-CaF_2. The Ce-doped samples were irradiated with X-rays (10000 mGy), prior to

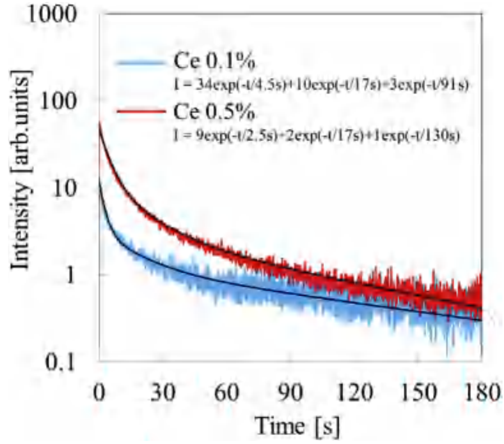

Fig. 7. OSL decay time profiles of Ce-doped $^{6}LiF/CaF_2$ after X-ray irradiation of 10000 mGy. The stimulation wavelength was 630 nm, and the monitoring wavelength was 335 nm.

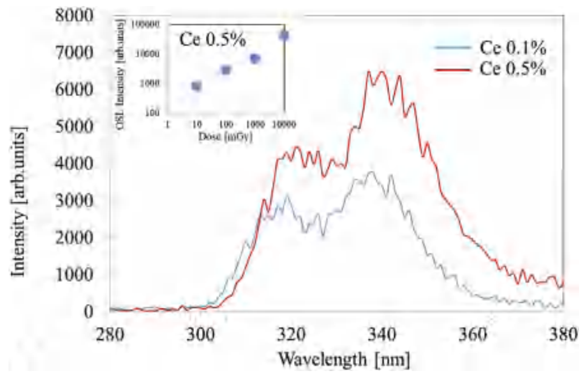

Fig. 8. OSL spectra of Ce-doped $^{6}LiF/CaF_2$ after X-ray irradiation of 1000 mGy. The stimulation wavelength was 630 nm.

the measurement. The stimulation wavelength was 630 nm, and the monitoring wavelength was 335 nm. The OSL signals decreased gradually during the stimulation, which was an evidence of OSL. Further, the decay time profiles were approximated by three exponential decay functions. The decay time constants of three components for the 0.1% Ce-doped sample were 4.5 s, 17 s and 91 s. In addition, the decay time constants of three components for the 0.5% Ce-doped sample were 2.5 s, 17 s and 130 s. These results suggested that at least three detrapping processes for OSL existed in the Ce-doped samples. Fig. 8 shows OSL spectra of Ce-doped $^{6}LiF-CaF_2$. The Ce-doped samples were irradiated with X-rays (1000 mGy) before the measurement. The Ce-doped samples showed emissions with peaks at 320 and 340 nm during the stimulation (630 nm). The emission wavelengths agreed well with those of 5 d-4f transitions of Ce^{3+} in PL. The OSL intensity of the 0.5% Ce-doped sample was higher than that of the 0.1% Ce-doped sample. Scintillation and OSL intensity had a complemental relation as well as TSL [32]. Furthermore, OSL dose response curve of the 0.5% Ce-doped sample was also shown in the set of Fig. 8. Here, OSL intensity represented the peak top value of the peak at 340 nm. The detected lower limit of the 0.5% Ce-doped sample was over 10 mGy, which was much higher than that of conventional OSL materials such as C-doped Al_2O_3 (1 μGy) and Tb-doped MgO (100 μGy) [4]. Therefore, Ce-doped LiF-CaF_2 eutectic compounds are a promising candidate for TSL material.

4. Conclusion

We investigated scintillation and dosimetric properties of Ce-doped $^{6}LiF-CaF_2$ eutectic compounds. As scintillation properties, the scintillation of the Ce-doped samples appeared at 300 nm and 320–340 nm due to the self-trapped excitons (STE) and the 5d-4f transitions of Ce^{3+} with typical decay times about 0.75 μs and 60 ns. Furthermore, the Ce-doped samples showed TSL glow peaks around 150 °C, and the 0.5% Ce-doped sample was confirmed to show linear response to the irradiated X-ray dose over a range of 0.1–1000 mGy. In addition, the Ce-doped samples also showed OSL with peaks at 320–340 nm due to the 5 d-4f transitions of Ce^{3+} during stimulation at 630 nm.

Acknowledgement

This work was supported by Grant-in-Aid for Scientific Research (A) (17H01375), Grant-in-Aid for Young Scientists (B) (17K14911) and Grant-in-Aid for Research Activity Start-up (16H06983) from the Ministry of Education, Culture, Sports, Science and Technology of the Japanese government (MEXT) as well as A-STEP from Japan Science and Technology Agency (JST). The Cooperative Research Project of Research Institute of Electronics, Shizuoka University, Mazda Foundation, Konica Minolta Science and Technology Foundation, NAIST Foundation and TEPCO Memorial Foundation are also acknowledged.

References

[1] S. Yamamoto, K. Kuroda, M. Senda, Scintillator selection for MR-compatible gamma detectors, IEEE Trans. Nucl. Sci. 50 (2003) 1683–1685.
[2] T. Yanagida, Y. Fujimoto, S. Kurosawa, K. Kamada, H. Takahashi, Y. Fukazawa, M. Nikl, V. Chani, Temperature dependence of scintillation properties of bright oxide scintillators for well-logging, Jpn. J. Appl. Phys. 52 (2013) 076401.
[3] J. Glodo, Y. Wang, R. Shawgo, C. Brecher, R.H. Hawrami, J. Tower, K.S. Shah, New developments in scintillators for security applications, Phys. Procedia 90 (2017) 285–290.
[4] B.C. Bhatt, Thermoluminescence, optically stimulated luminescence and radiophotoluminescence dosimetry: an overall perspective, Radiat. Protect. Environ. 34 (2011) 6–16.
[5] A.J.J. Bos, High sensitivity thermoluminescence dosimetry, Nucl. Instrum. Methods. Res Sect B 184 (2001) 3–28.
[6] N. Kawano, T. Kato, G. Okada, N. Kawaguchi, T. Yanagida, Optical, scintillation and dosimeter properties of MgO: Tb translucent ceramics synthesized by the SPS method, Opt. Mater. 73 (2017) 364–370.
[7] T. Yanagida, Y. Fujimoto, M. Koshimizu, N. Kawano, G. Okada, N. Kawaguchi, Comparative studies of optical and scintillation properties between $LiGaO_2$ and $LiAlO_2$ crystals, J. Phys. Soc. Jpn. 86 (2017) 092401.
[8] F. Nakamura, T. Kato, G. Okada, N. Kawaguchi, K. Fukuda, T. Yanagida, Scintillation and dosimeter properties of CaF_2 transparent ceramic doped with Eu^{2+}, Ceram. Int. 43 (2017) 604–609.
[9] T. Yanagida, M. Koshimizu, G. Okada, T. Kojima, J. Osada, N. Kawaguchi, Comparative study of nondoped and Eu-doped SrI_2 scintillator, Opt. Mater. 61 (2016) 119–124.
[10] T. Yanagida, N. Kawaguchi, Y. Fujimoto, K. Fukuda, Y. Yokota, A. Yamazaki, K. Watanabe, J. Pejchal, A. Uritani, T. Iguchi, A. Yoshikawa, Basic study of europium doped $LiCaAlF_6$ scintillator and its capability for thermal neutron imaging application, Opt. Mater. 33 (2011) 1243–1247.
[11] Y. Shimizu, M. Minowa, W. Suganuma, Y. Inoue, Dark matter search experiment with CaF_2(Eu) scintillator at Kamioka Observatory, Phys. Lett. B 633 (2006) 195–200.
[12] R. Hazama, S. Ajimura, H. Hayakawa, K. Matsuoka, H. Miyawaki, K. Morikubo, N. Siziki, T. Kishimoto, Scintillation efficiency of nuclear recoils in a CaF_2(Eu) crystal for dark matter search, Nucl. Instrum. Methods. Res Sect A 482 (2002) 297–303.
[13] M. Danilkin, A. Lust, M. Kerikmäe, V. Seeman, H. Mändar, M. Must, CaF_2:Mn extreme dosimeter: effects of Mn concentration on thermoluminescence mechanisms and properties, Radiat. Meas. 41 (2006) 677–681.
[14] A. Choujyakh, F. Gimcno, J.I. Pena, L. Contreras, V.M. Orera, Thermoluminescence properties of CaF_2-LiF: Mn eutectic melt grown composites, Phys. Chem. News 13 (2003) 139–143.
[15] J. Trohan-Piegza, J. Glodo, V.K. Sarin, $CaF_2(Eu^{2+})$:LiF – structural and spectroscopic properties of a new system for neutron detection, Radiat. Meas. 45 (2000) 163–167.
[16] N. Kawaguchi, K. Fukuda, T. Yanagida, Y. Fujimoto, Y. Yokota, T. Suyama, K. Watanabe, A. Yamazaki, A. Yoshikawa, Fabrication and characterization of large size $^{6}LiF/CaF_2$:Eu eutectic composites with the ordered lamellar structure, Nucl. Instrum. Methods. Res Sect A 652 (2011) 209–211.
[17] T. Yanagida, N. Kawaguchi, Y. Fujimoto, K. Fukuda, K. Watanabe, A. Yamazaki, A. Uritani, Scintillation properties of LiF–SrF_2 and LiF–CaF_2 eutectic, J. Lumin. 144 (2013) 212–216.
[18] T. Yanagida, K. Fukuda, Y. Fujimoto, N. Kawaguchi, S. Kurosawa, A. Yamazaki,

K. Watanabe, Y. Futami, Y. Yokota, J. Pejchal, A. Yoshikawa, A. Uritani, T. Iguchi, ^{6}LiF-SrF_2 doped with Eu eutectic scintillators for neutron detection, Opt. Mater. 34 (2012) 868–871.
[19] V.Y. Chekhovskoi, Thermal expansion and density of 80.5% LiF-19.5% CaF_2 eutectic, High Temp. 38 (2000) 197–202.
[20] L. Massot, P. Chamelot, M. Gibilaro, L. Cassayre, P. Taxil, Nitrogen evolution as anodic reaction in molten LiF-CaF_2, Electrochim. Acta 56 (2011) 4949–4952.
[21] C. Nourry, P. Soucek, L. Massot, R. Malmbeck, P. Chamelot, J.P. Glatz, Electrochemistry of uranium in molten LiF-CaF_2, J. Nucl. Mater. 430 (2012) 58–63.
[22] M. Chandra, S. Vandarkuzhali, S. Ghosh, N. Gogoi, P. Venkatesh, G. Seenivasan, B.P. Reddy, K. Nagarajan, Redox behaviour of cerium (III) in LiF-CaF_2 eutectic melt, Electrochim. Acta 58 (2011) 150–156.
[23] T. Yanagida, Y. Fujimoto, K. Watanabe, K. Fukuda, N. Kawaguchi, Y. Miyasaka, H. Nanto, Scintillation and optical stimulated luminescence of Ce-doped CaF_2, Radiat. Meas. 71 (2014) 162–165.
[24] T. Yanagida, K. Kamada, Y. Fujimoto, H. Yagi, T. Yanagitani, Comparative study of ceramic and single crystal Ce:GAGG scintillator, Opt. Mater. 35 (2013) 2480–2485.
[25] T. Yanagida, Y. Fujimoto, T. Ito, K. Uchiyama, K. Mori, Development of X-ray induced afterglow characterization system, APEX 7 (2014) 062401.
[26] T. Yanagida, Y. Fujimoto, N. Kawaguchi, S. Yanagida, Dosimeter properties of AlN, J. Ceram. Soc. Jpn. 121 (2013) 988–991.
[27] F. Nakamura, T. Kato, G. Okada, N. Kawaguchi, K. Fukuda, T. Yanagida, Scintillation and storage luminescence properties of MgF_2 transparent ceramics doped with Ce^{3+}, Opt. Mater. 72 (2017) 470–475.
[28] T. Yanagida, G. Okada, K. Fukuda, K. Watanabe, N. Kawaguchi, Optically and thermally stimulated luminescence of Ce- and Eu-doped $LiSrAlF_6$ crystals, Radiat. Meas. 106 (2017) 124–128.
[29] F. Nakamura, T. Kato, G. Okada, N. Kawaguchi, K. Fukuda, T. Yanagida, Scintillation and dosimeter properties of CaF_2 translucent ceramic produced by SPS, J. Eur. Ceram. Soc. 37 (2017) 1707–1711.
[30] V.A. Skuratov, S.M. Abu AlAzm, V.A. Altynov, Luminescence of aggregate centers in lithium fluoride irradiated with high energy heavy ions, Nucl. Instrum. Methods. Res Sect B 191 (2002) 251–255.
[31] D. Nakauchi, G. Okada, Y. Fujimoto, N. Kawano, N. Kawaguchi, T. Yanagida, Optical and radiation-induced luminescence properties of Ce-doped magnesium aluminoborate glasses, Opt. Mater. 72 (2017) 190–194.
[32] T. Yanagida, Ionizing radiation induced emission: scintillation and storage-type luminescence, J. Lumin. 169 (2016) 544–548.
[33] G. Kitis, J.M. Gomes-Ros, J.W.N. Tuyn, Thermoluminescence glow-curve deconvolution functions for first, second and general orders of kinetics, J. Phys. D Appl. Phys. 31 (1998) 2636–2641.